physica status solidi rrl

www.pss-rapid.com

Adsorbate-Induced Modifications in the Optical Response of the Si(553)–Au Surface

Sandhya Chandola, Simone Sanna, Conor Hogan, Eugen Speiser, Julian Plaickner, and Norbert Esser**

The conductivity of substrate-supported metallic nanowires can be adjusted, e.g., by strain or adsorbates. In this article, the effect of atomic hydrogen and toluene-3,4-dithiol (TDT) adsorption on the quasi-1D structures of the Si(553)-(5 × 2)–Au reconstruction is investigated. Reflectance anisotropy spectroscopy (RAS) and infrared ellipsometry reveal optical signatures of the surface. Spectral modifications related to the adsorbate exposure suggest the activation of adsorption-induced interband transitions. Density functional theory (DFT) calculations reproduce the spectral modifications and explain their origin. Preferential adsorption on sites located at the step edges of the structure occurs independent of the type of adsorbate and induces a charge transfer between electronic states related to the step edges and the Au dimer rows. This charge redistribution modifies the electronic structure close to the Fermi level, enhances the dimerization of the Au chains, and strongly influences the low-energy region of the RAS spectra. While previous studies employed atomic H as a chief adsorbate, it is shown here that even molecular H deeply modifies the Si(553)–Au optical response. Structural modification of Au–Si(553) by H and TDT adsorbates as suggested from recent ab initio calculations are verified.

1. Introduction

Deposition of metal atoms on selected semiconducting surfaces leads to a variety of ordered, atomic-scale chain structures.[1–11] Au-induced reconstructions on vicinal Si(111) surfaces have been studied intensively for years, as small coverages of Au stabilize the Si terraces by the formation of Au rows, which are expected to feature exciting physical properties such as quantization of conductance, spin-charge separation, charge and spin density waves, and Luttinger liquid behavior.[12–16] The Si(553)-(5 × 2)–Au surface was first investigated by Crain et al.,[17] and reported to show metallic states in the electronic band structure by angle-resolved photoemission spectrosopy. Since then, numerous lines of research have emerged, dedicated to the investigation of the atomic structure,[18–21] lattice dynamics,[22] spin patterns,[23–25] phase transitions,[26,27] as well as electronic structure and its adsorption-induced modifications.[28–32]

According to our current knowledge of the system, the high-temperature phase of the Si(553)–Au surface is stable from room temperature down to about 120 K. It consists of a double Au

S. Chandola
Division Energy and Information
Helmholtz-Zentrum Berlin für Materialien und Energie GmbH
Hahn-Meitner-Platz 1, 14109 Berlin, Germany
E-mail: sandhya.chandola@helmholtz-berlin.de

S. Sanna
Institut für Theoretische Physik and Center for Materials Research (LaMa)
Justus-Liebig-Universität Giessen
Heinrich-Buff-Ring 16, D-35392 Giessen, Germany

C. Hogan
Istituto di Struttura della Materia
Consiglio Nazionale delle Ricerche (ISM-CNR)
Via del Fosso del Cavaliere 100, 00133 Rome, Italy

The ORCID identification number(s) for the author(s) of this article can be found under https://doi.org/10.1002/pssr.202200002.

DOI: 10.1002/pssr.202200002

C. Hogan
Dipartimento di Fisica
Università di Roma "Tor Vergata"
Via della Ricerca Scientifica 1, 00133 Rome, Italy

E. Speiser
Laytec AG
Seesener Str. 10-13, 10709 Berlin, Germany

J. Plaickner
Division Energy and Transformation
Helmholtz-Zentrum Berlin für Materialien und Energie GmbH
Hahn-Meitner-Platz 1, 14109 Berlin, Germany

N. Esser
Technische Universität Berlin
Institut für Festkörperphysik
Hardenbergstr. 36, 10623 Berlin, Germany
E-mail: norbert.esser@isas.de

N. Esser
Leibniz-Institut für Analytische Wissenschaften -ISAS- e.V.
Schwarzschildstr. 8, 12489 Berlin, Germany

chain with dimerized Au atoms running parallel to the step edges in the middle of the terrace, and a honeycomb chain (HC) structure at the step edges (see **Figure 1**a).[18] The dimerized Au chains explain the ×2 periodicity observed, e.g., in electron diffraction experiments.[24,33] At lower temperatures, an additional ×3 periodicity is observed by electron diffraction as well as by scanning tunneling microscopy (STM).[34] It was first explained by distortions attributed to Peierls instabilities. However, density functional theory (DFT) calculations[23] subsequently suggested that the ×3 periodicity may arise from spin ordering, due to spin polarization at every third Si step-edge atom. Recently, it was shown that the low-temperature ground state of the ideal Si(553)–Au surface is actually diamagnetic: instead of a spin-polarized step edge, all dangling bonds of the step-edge atoms either host spin-paired electrons or are empty.[19] Structural phase transitions between the diamagnetic,[19] spin-polarized[24] and the double-chain model[18] have been predicted for increasing temperatures by ab initio molecular dynamics.[26]

Changes in the geometry, electronic structure, and optical properties of the Si(553)–Au surface as a function of adsorbate deposition have been predicted with the help of DFT calculations and observed experimentally.[28,33,35–37] Atomic or molecular adsorption is known to induce a surface charge redistribution between the step edge and Au-chain, which finds experimental support, e.g., by reflectance anisotropy spectroscopy (RAS) measurements during hydrogenation.[28,33,38]

In this work, we explore the impact of two different types of adsorbates that have been the subject of a previous ab initio calculation study: molecular H and toluene-3,4-dithiol (TDT), an aromatic divalent thiol with two -SH ligands. Atomic hydrogen is often used for surface modification, since it may easily terminate dangling bonds at the surface. Here, we use molecular hydrogen instead and show that it effectively works in a similar way, being catalytically decomposed to some extent at the surface. Therefore, no molecular pre-dissociation is needed, as already shown in our previous work.[28] Since some amount of H_2 is present in any ultrahigh vacuum (UHV) environment as the main component of the residual gas, the interaction with H may thus change this surface unintentionally. The organic molecule TDT is chosen in an attempt to induce a site-specific surface modification by selective adsorption to distinct surface sites than those known from hydrogen, which adsorbs preferentially to step edge sites.[28] TDT is chosen due to the presence of the thiol ligand which is well-known to bind to metal surfaces such as gold, opening up the possibility of selective metal–organic binding on the atomic Au chains via the S—Au bonds. TDT has two such -SH groups so that the molecule–surface interaction and site-specificity are enhanced—with respect to intermolecular interactions—by removing the extra rotational degree of freedom.

To this end, we measure RAS and IR optical spectra as a function of the adsorbate deposition time and perform corresponding ab initio calculations of the optical response. Figure 1b,c shows calculated structures with atomic H and TDT adsorbed at the step edges and at the honeycomb chains, respectively, from ab initio DFT calculations.[38] According to these calculations, TDT should initially adsorb preferentially at the step edge, very similar as suggested for H. At higher coverages, after saturation of the step edge sites, it is predicted to adsorb on the HC.[38] Moreover, in ref.[38] the surface electronic band structures were calculated for H and TDT adsorbate structures-in addition to the clean surface—i.e., with fully H-passivated step edge, with TDT and H passivated step edge and with H passivated step edge plus additional TDT on terrace sites. The electronic band structures show characteristic changes related to adsorbate modification, dependent in particular on the adsorption site. The band structures of the H or H/TDT passivated step edge structures were almost identical.

On the basis of the suggested structures from ref.[38] RAS and IR should give experimental evidence for the predicted structures and in particular the corresponding electronic surface band structures from ab initio calculations.

Versatile optical techniques such as RAS and infrared spectroscopic ellipsometry (IRSE), which are surface and polarization sensitive, offer precise microscopic information on the structural

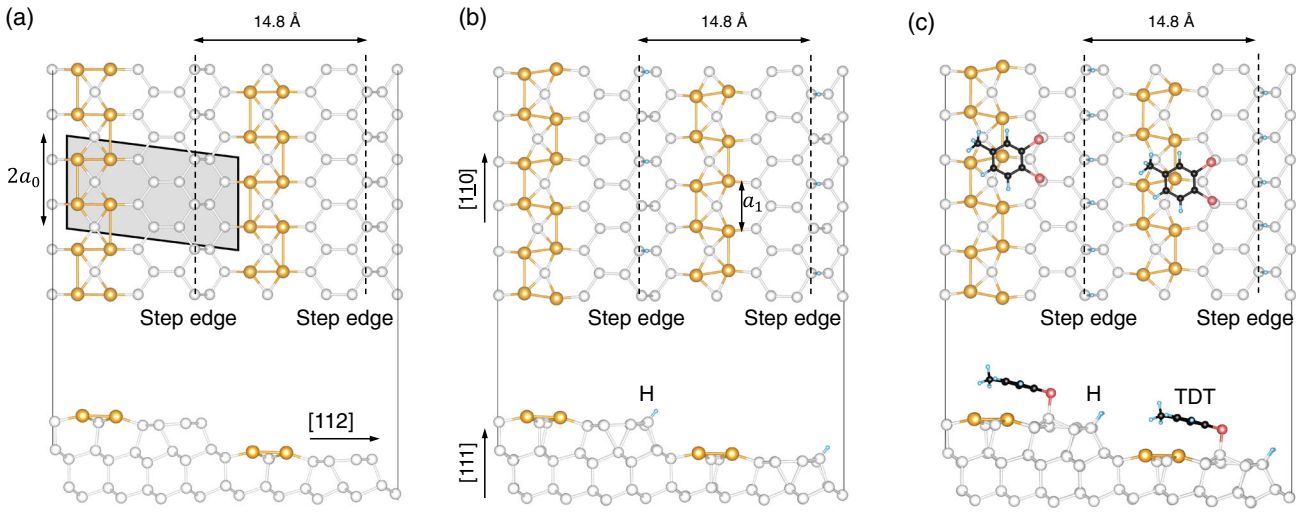

Figure 1. Structural models of the high-temperature phase of: a) the clean Si(553)-(5 × 2)–Au surface, and b) after adsorption of H and H, and c) toluene-3,4-dithiol (TDT), see ref. [38].

and electronic properties of nanometer-scale structures. IRSE is very sensitive to changes in the structural and electronic properties of quasi-1D systems,[39] as it monitors the band structure near the Fermi level. RAS has already proven to be a very useful technique for studying Si–Au surfaces, as it allows to establish a direct relationship between specific spectral features and structural elements of the surface, due to its sensitivity to local geometry.[40,41] A combination of DFT simulations and RAS[28,38] has been employed to show that the electronic properties of the Si(553)–Au system can be controlled by means of adsorbates such as H, which we also investigate in the present work. Yet, the optical response of the Si(553)–Au system in the low energy region below 1.5 eV is far from being understood. The main focus of this article is, therefore, set on the near-infrared energy region.

We demonstrate that optical measurements are sufficiently sensitive to monitor the changes in surface properties as induced by molecular H_2,[28,42] which we use instead of atomic H, in contrast to previous experiments.[33,35,37] Corresponding DFT-based calculations model the experiment. We should note that due to computational limitations the DFT-based calculations of the optical response are limited to the optical anisotropy. The IR ellipsometry measurements give additional information on the optical response in the MIR spectral range (below the Si bandgap), where surface optical transitions should also arise. Spectral features are observed as a function of H or TDT coverage, and are attributed to electronic transitions that are produced by H and TDT adsorption, due to changes in the surface band structure. The adsorption-induced signatures are related to a rearrangement of the electronic structure close to the Fermi energy. These are the result of charge transfer within the surface states, induced by the local chemical interaction of the adsorbates with certain states, and involve Si step edge states as well as Au-related states. Modifications of the latter lead to a strong enhancement of the Au chain dimerization, which supports previous studies showing strong cross-coupling between the electronic and structural properties.[33] TDT is found to adsorb preferentially on the step edges, and subsequently, after passivation of the step edge dangling bonds, on the Si honeycomb structure, similar to observed for H. This proves the result of the ab initio calculation that TDT does not interact strongly with the Au chain sites, in spite of its S–H functional groups which are known to react strongly with Au surfaces.

2. Results and Discussion

2.1. Hydrogen Adsorption

2.1.1. RAS Investigation of the Clean and Adsorbed Si(553)–Au Surface

Figure 2 shows the H-induced modifications of the optical properties of the Si(553)–Au surface. Strong adsorption-induced modifications of the optical response are evident in the IR and up to the UV spectral range. Both IR and RAS spectra clearly show spectral features that are related to surface electronic transitions, as discussed in the following, starting with the RAS part. The RAS measurement of the clean Si(553) surface is shown in Figure 2b (black dotted curve). The spectrum is mostly flat, with well-known features occurring at E_1 and E_2 gaps of Si from step-edge-modified bulk-like optical transitions. After Au deposition, a well-ordered Si(553)–Au surface is formed, as confirmed by room-temperature low energy electron diffraction (LEED) images with ×2 streaks[28] (not shown here). The corresponding Si(553)–Au RAS spectrum (gold curve) is characterized by a strong minimum at about 2.0 eV, and a shoulder at about 2.7 eV.[28] A slight dip between 1.2 and 1.3 eV can also be seen. In addition, a broad positive structure at about 1 eV is visible. According to previous calculations of different vicinal Si(*hhk*)–Au surfaces, the RAS feature at 2 eV arises from transitions between states localized at the Si step edge and the Au chain, while the transition at 2.7 eV is localized in the back part of the honeycomb structure.[43] The structure at 1.0 eV has been previously associated with the Au chain dimerization, instead.[40] The measured features are unambiguously related to surface states, as this energy region is far below the direct

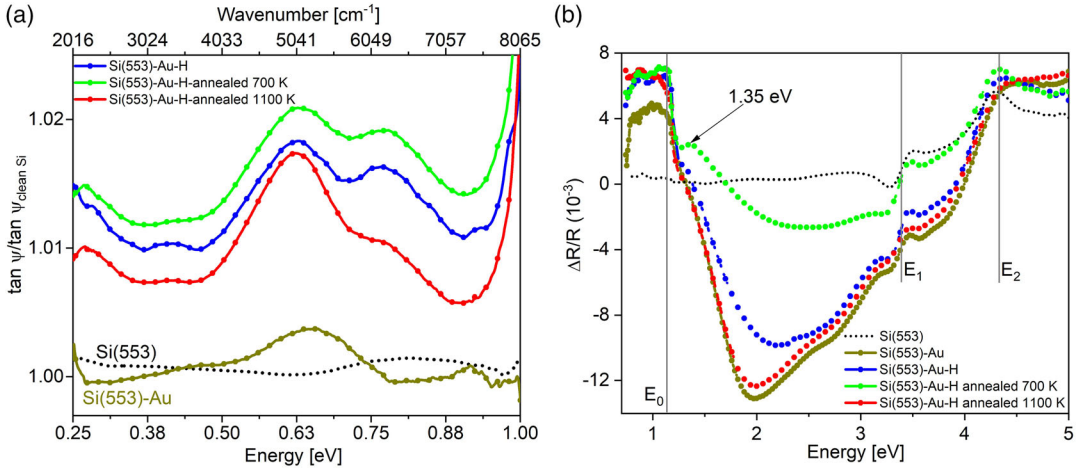

Figure 2. a) Infrared ellipsometry of the clean and hydrogenated Si(553)–Au surfaces before and after thermal treatment. Measurements are performed with the plane of incidence perpendicular to the Au chains. b) Reflectance anisotropy spectra of the same surface. Spectral signatures of the IR and RAS spectra are related to electronic transitions of the surface. The critical points in Si are marked as E_0 (indirect gap), and E_1, E_2 (direct gaps).

optical gap of Si (E_1 gap at 3.4 eV). RAS measurements performed at low temperature (70 K, not shown in this work) are very similar, except for a slight sharpening of the 2 eV minimum, suggesting that the signal could originate from strongly localized states.

RAS measured on the hydrogenated Si(553)–Au surface (i.e., after exposure to H_2, up to 1000 L) is shown in Figure 2b, (blue curve). While the optical anisotropy at 2.0 eV (step edge related) exhibits a decrease in intensity, the optical anisotropy at 2.7 eV (honeycomb related) is not as strongly affected. This is compatible with H adsorption at the step edge, as represented in Figure 1b and in agreement with previous findings.[28,35] A two-stage adsorption process has been monitored with RAS,[28] with the dangling bonds at the step edges being the most stable adsorption site, followed by adsorption at the terraces. Atomistic models have furthermore shown that the effect of H adsorption on the honeycomb chains is negligible, while the dimerization of the Au chain is enhanced by electronic charge transfer.[28,33,35] The small dip between 1.2 and 1.3 eV becomes more visible, while the structure at 1 eV increases in intensity. In the LEED images of the hydrogenated surface (not shown here) the $\times 2$ streaks are clearly visible.

Annealing the surface at 700 K (green curve) strongly reduces the optical anisotropy between 1.2 and 3 eV. A small peak at 1.35 eV develops, and the dip becomes more defined. Annealing at a higher temperature (1100 K, red curve) recovers the anisotropy of the clean surface almost completely. This suggests that a temperature of 700 K is not sufficient to drive off H adsorbates (a temperature of about 900 K is usually needed to fully desorb H according to the literature). The surface after annealing at 700 K has thus to be interpreted as a disordered surface with partially recovered and partially still H passivated surface regions. Due to the dissociation of H_2 at the Si surface, partial coverage of H at the step edges is expected even after annealing.

The broad structure at 1 eV is not affected by annealing at 700 or 1100 K. The appearance of the peak at 1.35 eV could indirectly indicate an enhanced amplitude of Au dimerization, following recent findings that adsorption of hydrogen at the Si step edges enhances the dimerization parameter of the Au chains.[33] In a two-photon photoemission (2PPE) investigation of the Si(553)–Au surface,[44] transitions between initial states (0.93 and 0.79 eV) below the valence band maximum and intermediate states (0.62 and 0.76 eV) localized in the bandgap have been observed. These related optical transitions at about 1.5 eV contribute to the appearance of the RAS feature at 1.35 eV.

2.1.2. Comparison with Theoretical Results

As all RAS and IR measurements of the Si(553)–Au surface have been performed at room temperature, our calculations are based on the diamagnetic model by Krawiec.[18] Calculated RAS spectra of the clean and hydrogenated Si(553)–Au surface (as shown in Figure 1) are shown in **Figure 3**a,b, respectively. The RAS signal calculated for the clean surface (black curve) closely matches the experimental curve. The measured negative peak at 2.0 eV, as well as the signatures E_1 at about 3.5 eV and E_2 at about 4.5 eV are well reproduced in the calculations, although the whole spectrum is slightly red-shifted by about 0.5 eV due to the DFT- generalized gradient approximation (GGA) underestimation of the fundamental electronic bandgap. The only difference between measured and calculated spectra is the low energy peak measured at about 1 eV, which only appears in the simulation of the hydrogenated surface (Figure 3b light blue curve). This suggests the presence of H even in nominally clean samples. Indeed, even in experiments conducted in UHV, H (or

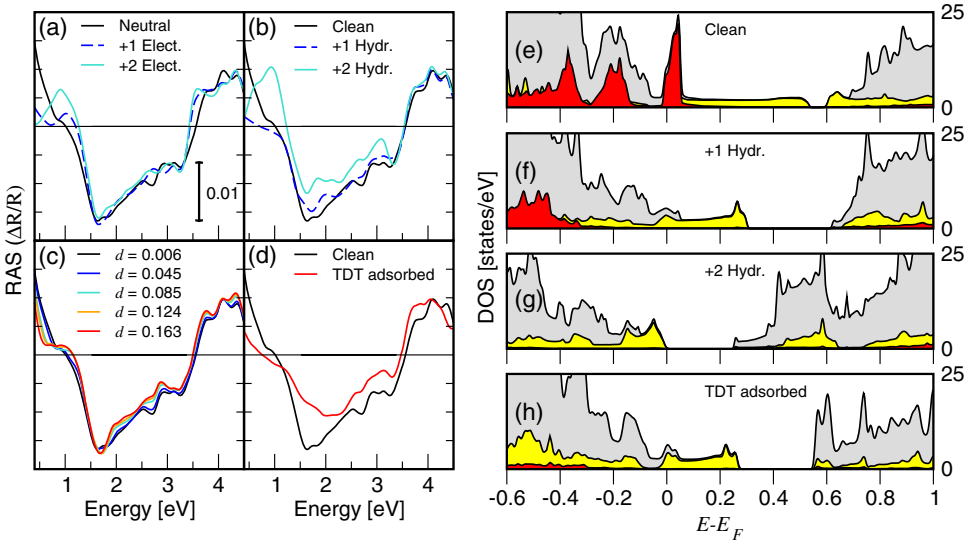

Figure 3. RAS spectra of the Si(553)–Au surface calculated within DFT- Perdew–Burke–Ernzerhof (PBEsol) as a function of: a) electron doping, b) H adsorption, c) Au chain dimerization, and d) TDT adsorption. The horizontal line marks the scale origin. Calculations are based on the structural model proposed by Krawiec,[18] which represents the room temperature phase. e) Corresponding site projected DOS calculated for a (5×2) unit cell within DFT–PBEsol for the clean Si(553)–Au surface, f) half, and g) fully H-saturated step edge, and h) after TDT adsorption. The total DOS is in gray; the contributions of the Au chain and of the Si step edge are represented in yellow and red, respectively.

residual gas) is always present, as it is very difficult to pump it away, so the "clean" Si(553)–Au surface probably has some amount of H adsorbed on it. We would like to emphasize that this holds for molecular H_2, which we used for dosing in our experiments, and which is always present in residual gas. By using atomic hydrogen the adsorption is much more rapid, but the according changes in the surface optical spectra are the same. Thus, we conclude that molecular hydrogen is decomposed on the surface to some extent but leads to the same adsorption structures after sufficient exposure time.

In our calculations, the H adsorption has only a minor effect on the surface structure, the main effect being the dimerization enhancement. It increases from $d = 0.006$ of the clean surface to $d = 0.111$ and $d = 0.196$ with one or two H atoms per (5×2) unit cell, respectively (see Equation (3) for the definition of d). Similar to the behavior observed in the measurements, the H adsorption diminishes the overall optical anisotropy, proportionally to the amount of adsorbed H. The intensity of the spectral feature at 1 eV increases with the H coverage, instead. The interpretation of this peak is not straightforward. In previous studies, it was associated with the dimerization of the Au chain.[28,40] Yet it might be due to adsorption-induced structural modifications of the step edge or of the Au chain (via charge transfer), or to a change of the electronic structure due to the adsorbate-to-substrate charge transfer.

To investigate this question, we calculated the RAS signal for a clean surface with additional electrons (see Figure 3a) at the corresponding equilibrium structure (i.e., performing a structural optimization after electron doping). As expected, electron injection enhances the dimerization of the Au chain from $d = 0.006$ of the clean surface to $d = 0.123$ and $d = 0.163$ with one or two electrons per (5×2) unit cell, respectively. Electron doping does not substantially modify the RAS spectrum above 1.5 eV, however, it leads to the formation of the low-energy RAS signature at about 1.0 eV. This excludes that the peak originates from the formation of Si–H bonds at the Si step edge, but does not reveal whether the peak is due to the enhanced dimerization of the Au chain or to a modification of the band occupation.

To understand the role of the chain dimerization in the RAS spectra, we artificially fix the chain dimerization at different values between $d = 0.006$ of the clean surface and $d = 0.163$, which is the dimerization resulting from doping with two electrons per (5×2) unit cell. The corresponding RAS calculations are shown in Figure 3c. Merely increasing the dimerization of the Au chain does not lead to the formation of the low-energy RAS peak. However, it enhances the dip measured at 1.25 eV and shoulder measured at 1.35 eV, respectively. Thus, the 1 eV peak is clearly related to the charge transfer between the step edge and Au chain structures, while the dip/peak structure around 1.25/1.35 eV is related to the dimerization parameter within the Au chains.

Figure 3d shows the calculated RAS for TDT adsorption at the terraces with step edge sites terminated by H. For TDT adsorption at the step edges, the RAS spectra should refer to the one with H adsorbed, since the calculated surface band structures were found to be essentially the same.[38] The curve is substantially flattened, as the flat TDT molecules affect the substrate anisotropy. The low-energy peak is not present, although the calculated Au dimerization is 0.134, which is similar to the one calculated for 2 additional electrons on the $(5 \times 2$ cell) or, almost equivalently, for a fully H adsorbed step edge. This confirms that the low-energy peak does not originate from the Au chain dimerization.

The analysis of the site's projected density of states (DOS) yields further insight into the mechanisms occurring upon adsorption. Figure 3e shows the DOS of the clean Si(553)–Au surface (in gray) as well as the contribution of the Au chain (in yellow) and of the step edge (in red). The step edge states are localized at the Fermi energy as well as in the valence band. The Au-related states are distributed over the whole energy range (partially covered by the step edge states), instead. The main effect of the H adsorption is to shift the step edge states well below the Fermi energy by electronic passivation after charge redistribution within the surface layer. At the same time, the bandgap between Au states in the conduction band is widened (Figure 3f). For a fully passivated step edge (Figure 3g), the step edge states are completely shifted into the valence band, and the system undergoes a metal-to-insulator transition, in agreement with ref. [38]. The TDT adsorption on an H passivated surface has a similar effect, although the surface remains metallic (Figure 3h). The similarity of the DOS in Figure 3f,h is mirrored by the corresponding RAS spectra (blue dashed curve and solid red curve in Figure 3b,d, respectively).

2.1.3. IR Investigation of the Clean and Hydrogenated Si(553)–Au Surface

The IR measurements in Figure 2a are made with the plane of incidence perpendicular to the Au chains, and taken simultaneously with the RAS measurements. The spectral range is cut off at 1 eV due to absorption from the beam splitter. The spectrum of the "clean" Si(553)–Au surface, before hydrogenation, shows a broad feature at about 0.64 eV ($5200\,cm^{-1}$). Accordingly, investigations of the Si(553)–Au surface with 2PPE[44] showed the presence of two unoccupied surface states in the bandgap at 0.62 and 0.76 eV. The band structure calculations[38] show that these surface states are related to both the step edges and the Au-chains, which are also seen in the site-projected DOS shown in Figure 3e. Overall, IR ellipsometry clearly reveals interband transitions below the fundamental bandgap of Si, indicating the participation of surface bands within the Si bulk gap.

Strong changes in the IR ellipsometric measurements are observed after H adsorption, with the appearance of several broad peaks due to the modification of the surface band structure by the adsorbates. More in detail, IR spectra of the hydrogenated surface (offset for clarity, blue curve) show that the broad feature increases in intensity, sharpens, and shifts slightly to 0.62 eV. A new peak at 0.77 eV ($6200\,cm^{-1}$), a weak broad structure at about 0.41 eV ($3300\,cm^{-1}$) as well as a feature at about 0.25 eV ($2000\,cm^{-1}$) appear. The peaks at 0.62 and 0.77 eV could originate from the same unoccupied states as observed in the 2PPE study,[44] and should be associated with surface interband transitions. The spectral feature in the region of 0.25 eV ($2000\,cm^{-1}$) partly arises from Si–H or a combination of Si–hydride stretching vibrations, but the interpretation is hampered by the presence of CO_2 absorption between 2300 and $2385\,cm^{-1}$ due to nonideal dry air purging of the spectrometer.

Band structure calculations of the H passivated Si(553)–Au surface[28,35,38] showed the creation of new states located at the Si honeycombs, with excess charge redistributed to the Au chains. This is accompanied with a number of surface bands arising in the Si bandgap close to the conduction band minimum. The appearance of the structures at about 0.41, 0.62, and 0.77 eV in the IR spectra could arise from interband transitions between these states. The changes in surface electronic structure imposed by the hydrogenation of the step edge states are clearly visible in the calculated DOS, shown in Figure 3f,g, which are in full agreement with the calculated band structures of ref.[38] While the step-edge related states are strongly shifted to lower binding energy upon H passivation, the according charge transfer also affects the Au-related surface states significantly. The modification of the Au-related surface states may, most likely, explain the changes in the IR spectra between 0.4 and 0.8 eV. The calculated RAS of the hydrogenated and electron-doped surface (see Figure 3a,b) also supports this interpretation, due to the appearance of features in the NIR region between 0.5 and 1 eV, which refer to changes in the surface band occupation.

In a recent study, hydrogen adsorption resulted in the opening of band gaps between Au bands due to an indirect charge transfer to the Au-related bands.[33,35] The magnitude of the bandgap was shown to be linearly related to the dimerization amplitude. From the combination of experimental results and DFT, it was found that this enhanced dimerization is strongly coupled to elementary charge donation to surface bands and the subsequent bandgap opening at an unoccupied state or relocation of the Fermi level. Thus the appearance of the peaks in the IR spectra upon hydrogenation is probably related to the enhancement of the dimerization of Au chains and electronic occupation of the related surface bands.

Annealing at 700 K (green curve) does not affect the peaks at 0.62 and 0.77 eV, but the weak broad feature at 0.41 eV is not visible anymore. Annealing at 1100 K (red curve) reduces the peak intensity at 0.77 eV with a corresponding increase in the intensity of the peak at 0.62 eV. The peak at 0.77 eV is most likely indicative of adsorbates on the surface. After annealing, the step edges are not fully clean, since residual gas reabsorbs on them. Therefore, the amplitude diminishes, but is not zero. Thus, annealing at 1100 K (which should desorb H) does not affect these two peaks drastically, except for a readjustment of the ratio of their amplitudes, indicative of possible electronic changes within the surface structure during annealing. From RAS measurements of hydrogenated Si(553)–Au surfaces, it is known that annealing the surface above 1000 K can recover the RAS signal,[28] and even improves the structural order. The sample is not moved during hydrogenation and annealing at different temperatures, with the optical measurements conducted in-situ and in real time during these processes.

2.2. TDT Adsorption

In another adsorption experiment, TDT is deposited on the Si(553)–Au surface. The effect of TDT on the local charge distribution is studied to probe whether TDT adsorption leads to more drastic changes on specific structural elements such as the step edges, honeycomb chains and the Au chains. Ab initio calculations of the minimum energy structures in ref.[38] have suggested that TDT should preferentially adsorb to the step edges, and after saturation, to Si honeycomb sites, while Au chain sites are unfavourable. Similar to the H adsorption, the IR and RAS spectra clearly show spectral features which are related to surface electronic transitions, and will be discussed, starting with the RAS part. **Figure 4**b shows RAS spectra of the Si(553)–Au surface before and after TDT deposition. The RAS spectra measured before TDT deposition as a function of the time after sample preparation, are called Si(553)–Au@T1, Au@T2, Au@T3. They show some quenching of surface states at the step edges (2 eV), very similar to that observed for H_2 adsorption, see Section 2.1.1. This is probably due to residual gases in the UHV chamber, (TDT fragments from previous TDT gas inlets), which passivate local dangling bonds at the step edges with increasing exposure time T1 to T3. The surface is then exposed to ≈50 L of TDT through a leak valve. The RAS curve appears flattened between 1.5 and 3 eV (green curve), in very good agreement with the calculations presented in Figure 3b. The optical anisotropy at 2 eV, related to the step edges and the shoulder feature at 2.7 eV (honeycomb related), are heavily attenuated, suggesting that surface states related to these structural features are significantly affected. The feature at 1 eV is almost completely quenched. Comparing the RAS of the hydrogenated surface in Figure 2 to RAS of the TDT adsorption, it is clear that TDT interacts chemically with electronic states related to different surface sites. As compared to H adsorption, a much broader minimum as well as a strong decrease in intensity at about 1 eV is observed. A dip at 1.2 eV and a small peak at 1.4 eV appear after exposure to TDT, almost at the same energies as for the H adsorbed surface, which shows that the 1 eV peak is related to the charge transfer between the step edge and Au chain structures, while the dip/peak structure is related to the dimerization parameter within the Au chains. RAS transients taken at 2 eV (sensitive to the dangling bond states at the step edges) as a function of H_2 and TDT exposure are shown in Figure 4c. It can be seen that the RAS amplitude during H_2 exposure (blue) is decreasing at a similar rate to the RAS (dark green) before the leak valve is opened for TDT dosing. The transient before H_2 exposure changes at a much slower rate, and is almost flat. The optical transitions involving the step edges are being quenched at the same rate for H adsorption as the surface, where residual TDT is in the chamber. After the leak valve is opened for TDT dosing, the amplitude attenuates rapidly, saturating at about 10 L. Higher exposures of TDT led to no further changes in the spectrum. This absence of a change indicates that ≈10 L exposure of TDT results in a fully saturated layer. For H_2 dosing, the amplitude decreases at a much slower rate, saturating between 300 and 400 L (the *x*-axis is cut off at 50 L to highlight the steep slope of the TDT exposure). LEED of the surface after TDT adsorption shows that the ×2 streaks are not visible, and the ×5 spots are very faint, indicating a disordered surface. The broad minimum and drastic reduction of anisotropy after TDT adsorption show that the interaction of TDT with different surface sites such as step edge sites and terrace sites is much stronger than in the case of H_2. The flattening of the RAS curve after TDT exposure, as well as the absence of the structure at 1 eV, is in very good agreement with the calculations in Figure 3d. The low energy peak is not present, although the

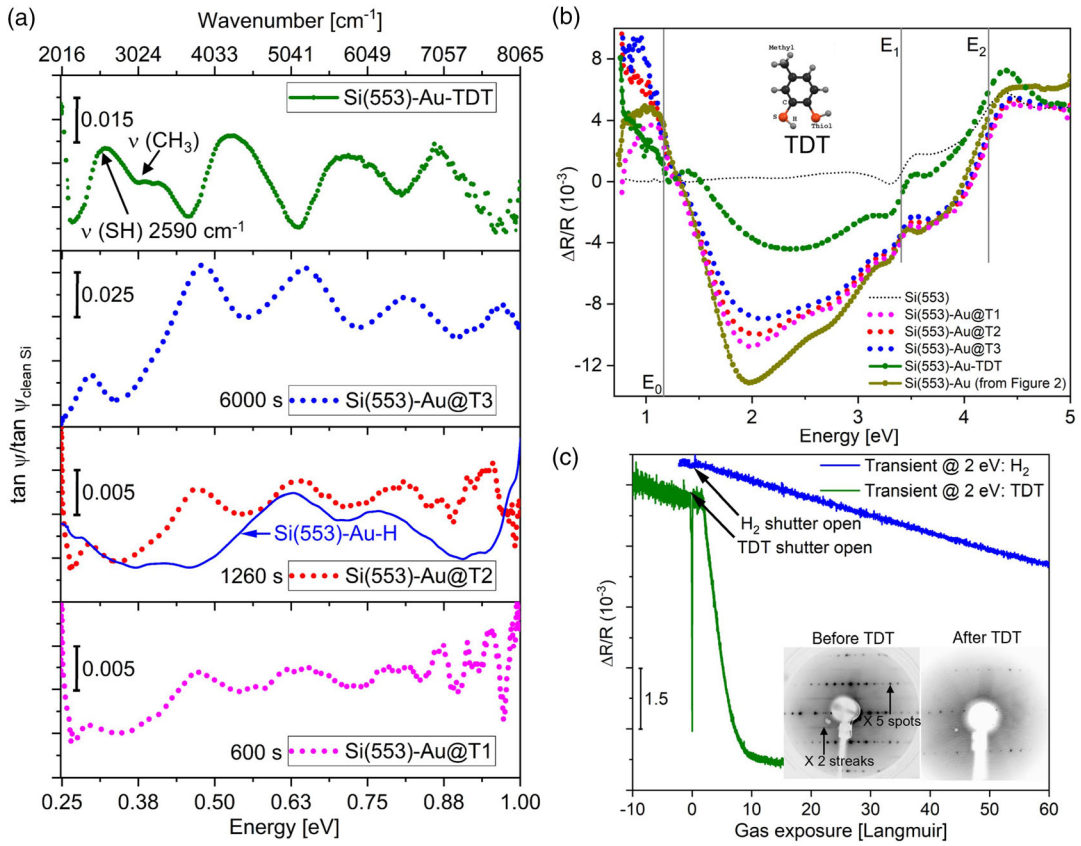

Figure 4. a) IR spectra, b) RAS spectra, and c) RAS transients of the Si(553)–Au surface dosed with TDT. The transient shows the RAS amplitude at 2 eV both for H_2 and TDT exposure. Low-energy electron diffraction (LEED) images of the clean Si(553)–Au surface and after 50 L of TDT are also shown. The sharpness of the ×5 diffraction spots and the high signal-to-background ratio indicate good sample quality and long-range order of the clean surface. The half-order horizontal streaks indicate the dimerization of the Au chains. After TDT exposure, the half-order streaks are not visible, showing that TDT has disturbed the long-range order of the Au chains and the intensity of the ×5 spots has reduced.

calculated Au dimerization is 0.134, which is similar to the one calculated for two additional electrons on the (5 × 2) cell or, almost equivalently, for a fully H-adsorbed step edge. This confirms that the low energy peak does not originate from the Au chain dimerization. The surface anisotropy is strongly affected by TDT adsorption. At higher coverages, in particular, TDT molecules cover a large part of the surface being adsorbed partly at the step edges (together with some amount of H), and partly at terrace sites.[45]

Infrared spectra, see Figure 4a, show the evolution of interband transitions in the lower energy range (sub-bandgap), as a function of time (Au@T1 to Au@T3) before TDT is deliberately dosed on the surface. The sample is not moved during the sequence of measurements. The amount of time in seconds, in each graph (600 s, 780 s, etc.) denotes the time from the Si(553)–Au growth. Broad peaks can be seen developing at 0.46, 0.64, 0.8, and 0.9 eV, recorded simultaneously with the RAS spectra. As mentioned earlier, there is residual TDT, hydrogen, and possibly hydrocarbons (from TDT fragments) present in the chamber, which is already sufficient to affect the reactive step edge sites on the surface. As mentioned in Section 2.1.3, the spectral feature in the region of 0.25 eV (2000 cm^{-1}) could partly arise from a combination of Si-hydride stretching vibrations, but the interpretation is hampered by the presence of CO_2 absorption between 2300 and 2385 cm^{-1}. As discussed in the previous section, the adsorption of H or TDT fragments does not lead to a disruption of the surface structure but induces a charge transfer between the step edge and Au-chain surface states, accompanied by a gradual change in the Au chain dimerization. The according sequence of IR spectra shows the appearance of a number of peaks, similar to the H-terminated step edge, with increasing amplitudes and slightly increasing peak energies with exposure time. We associate this to the modification of surface states induced by step edge termination and the charge transfer related to it. The gradual shift in transition energies with exposure time fits well with the theoretical prediction that adsorption at the step edges should result in an opening of band gaps between Au bands due to charge transfer to the Au-related bands[33,35] (see discussion in paragraph 2.1). It shows, overall, that the step edge sites of the clean Si(553)–Au surface are very reactive to various residual gas adsorbates (hydrogen, hydrocarbons, TDT fragments). Since no disruption of the overall structure occurs, the change in surface electronic properties is governed by charge transfer in all these cases. The gradual increase in amplitudes of the peaks as time progresses suggests a corresponding increase of the amount of residual TDT adsorbed on the surface until it

saturates at about 6000 s. The spectrum of the hydrogenated Si(553)–Au surface from Figure 2a is plotted (dark blue line) along with the spectrum taken at 1260 s in Figure 4a. The broad peak at 0.62 eV for the hydrogenated surface is almost at the same energy but the structures at 0.41 and 0.77 eV are shifted to 0.46 and 0.8 eV and develop in intensity with the appearance of an additional peak at 0.9 eV. 2PPE measurements of the Si(553)–Au surface[44] showed the presence of two occupied states at 0.79 and 0.93 eV. Almost identical band structures were calculated for hydrogen adsorption and TDT adsorption at step edges (ref. [33]), though the theoretical predictions are for ideal surfaces, whereas experimentally, residual TDT fragments can adsorb not only at step edges but on various defect sites on the surface which could contribute to slight changes in the electronic structure.

Distinct changes in the spectra occur with additional TDT on the surface. After 50 L of TDT dosage, a broad feature appears at about 2590 cm^{-1} (dark green curve in Figure 4a). Several other broad peaks also appear, which are shifted toward higher energies compared to the spectra before TDT dosing. The results were compared to a standard IR transmittance spectrum of gas-phase TDT (from NIST Chemistry WebBook). Pure TDT shows a strong S–H vibrational mode at ≈2560 cm^{-1}. The absence of this mode would imply the formation of a new chemical bond involving both sulfur atoms in the TDT molecule, which are no longer terminated by hydrogen. The broad IR feature at 2590 cm^{-1} could then be a weak S–H vibrational feature, which implies that the S—H bond is not fully cleaved upon adsorption, with the presence of some TDT fragments. Overall, TDT adsorbs in a less well-ordered fashion compared to hydrogen. Nevertheless, for low exposures, step edge sites are initially involved (according to the very similar RAS spectra in both cases), while at higher TDT exposures terrace sites are affected. Small vibrational features are also seen around 3080 cm^{-1} which could arise from CH_3 fragments of the molecules.

In a Raman and DFT study of the adsorption of TDT on Ag islands,[46] a broad band was calculated at about 2550 cm^{-1}. This feature was related to several components of the S–H band of the thiol group with a broadening and shift toward lower energies due to the increased amount of dimerized molecules in the TDT molecule from possible exposure to ambient light. The feature measured at 2590 cm^{-1} could thus originate from S–H stretching vibrations, which are broadened due to adsorption of partially disordered layers of TDT on the surface as well as the formation of dimerized or polymerized TDT. In a surface-enhanced Raman spectroscopy (SERS) study of 1,4-benzenedithiol (1,4-BDT) adsorbed on Au surfaces,[47] the spectral pattern was dependent on the concentration of 1,4-BDT. At low coverages of BDT, the S–H stretching bands were barely detected in the SERS spectrum. On increasing the concentration of 1,4-BDT, bands appeared around 2555 cm^{-1}. It was suggested that the orientation of 1,4-BDT on Au is dependent on the surface coverage. When the surface coverage is very low, BDT assumes a rather flat orientation while at higher coverages the adsorbate takes on a perpendicular orientation. The observation of the broad band at 2590 cm^{-1} in the IR spectra of TDT could be due to the orientation of the TDT molecules which align perpendicular to the surface.

Referring to the calculations for TDT adsorption on an H passivated surface (Figure 1c), the terrace sites are the next most stable adsorption site after the step edges are blocked, so the molecule disrupts the honeycomb chains, breaking the double Si bonds, with half of the empty honeycomb states disappearing. According to the calculated DOS in Figure 3h, the IR spectral features could arise from the related Au bands, similar to the discussion for H adsorption. TDT adsorption on the honeycomb sites disturbs the charge balance of the step edge-passivated (nonmetallic) surface structure. The resulting shifts in the Fermi level and in the Au-related bands should give rise to changes in the IR spectra. While there may also be contributions from the honeycomb states, the changes in the Au chain state energy and occupation already explain the observed IR signal very well. The large quantity of TDT has probably perturbed the entire surface, including the honeycomb structure, causing the electronic structure to be significantly changed. The RAS signature of the Si(553)–Au surface exposed to TDT is still essentially visible, though it now resembles a structure that is capped by a molecular layer, and shows that the Au nanowire structure is still intact.

3. Conclusion

The optical response of the Si(553)–Au surface is monitored as a function of H and TDT coverage with RAS and infrared ellipsometry. For the Si(553)–Au system, the electronic and structural properties are strongly intertwined in a specific way. This correlation is observed in the spectral features that develop upon the transfer of charge to Si and Si–Au surface states, associated with adsorbate attachment. The optical spectra are attributed mostly to surface-related electronic interband transitions that are modified by H or TDT adsorption. Strong modifications are seen in the near-infrared and visible spectral range which are related to changes in the surface band occupation due to electronic charge transfer from edge states to Au chain states. DFT calculations agree well with the measured spectral modifications and indicate an enhancement of the dimerization parameter of Au chains. The presence of H has a strong influence on the adsorption geometry of the TDT molecules. The latter adsorb at the step; however, they adsorb on the terraces if the Si step edge is already adsorbate passivated. Thus, changes are observed in the surface optical spectra, related to the adsorption of H or TDT at the step edge and TDT at the terraces. The accompanying charge transfer is the dominant source of changing surface electronic properties, while the structure itself is only slightly affected. Higher coverages of TDT modify the honeycomb structure; however, the Au nanowire structure is still intact as seen by the persistent, broad RAS signal. The optical response in the IR spectral region is sensitive to subtle modifications in the surface bandstructure, even with the use of molecular H.

4. Methodology

4.1. Experimental Section

The experiment was carried out in an UHV chamber, base pressure 1×10^{-10} mbar, equipped with LEED, effusion cells, sputter

gun, gas inlet lines, annealing and cooling sample stages, and in situ IR, UV–vis optics. The Si(553) sample was n-type, phosphorous doped, with a resistivity in the range of 0.01–0.1 Ω cm. Direct current heating of the sample up to 1250 °C produced a regular array of single height steps, with LEED showing long-range order. Gold was deposited on the clean Si(553) surface at an elevated substrate temperature of 650 °C followed by post-annealing at 950 °C for 10 s. The optimum gold coverage was recently shown to be 0.48 ML, with 2 gold atoms per primitive unit cell as opposed to earlier work, which assumed a coverage of 0.25 ML. The ×2 streaks were visible in LEED at room temperature. In the RAS measurements, the reflectance R, at near-normal incidence, of light linearly polarized in two orthogonal directions are measured.[48] The RAS signal is defined by

$$\frac{\Delta R}{R} = \frac{R_{[\bar{1}10]} - R_{[11\bar{2}]}}{R} \tag{1}$$

where the directions $[\bar{1}10]$ and $[11\bar{2}]$ correspond to directions parallel and perpendicular to the steps, respectively. All RAS spectra in this work reported the real part of the anisotropy in the reflection coefficients $\Delta r/r$, which is related to the signal by $\Delta R/R = 2Re(\Delta r/r)$.

IR measurements used an ellipsometer attached to a Bruker Vertex 70 series Fourier Transform Interferometer with a spectral resolution of 16 cm^{-1} (2 meV). Ellipsometry measured the changes in the polarization state of linearly polarized incident light upon reflection from the sample surface. This change is expressed as the ratio of the complex Fresnel reflection coefficients r_p and r_s for light polarized parallel and perpendicular to the plane of incidence. The measurements were performed in reflection at 65° angle of incidence and the polarization state of the reflected radiation was analyzed. The ellipsometric parameters, ψ and Δ, are related to the complex reflection coefficients for polarization perpendicular and parallel to the plane of incidence, r_s and r_p, by $r_p/r_s = \tan\psi \exp(i\Delta)$. Only $\tan\psi$ was measured, as a retarder was not available to measure the phase difference Δ. Measurements of the clean Si surface at room temperature (RT) were used to normalize the results. The Si(553)–Au surface was exposed to molecular hydrogen at room temperature. The UHV chamber was back filled with ultrapure H_2 through a leak valve. The H_2 and TDT dosage in the sample was varied by the gas pressure and exposure time. The pressure ion gauge was switched off to avoid H_2 dissociation at the ion filament.

4.2. Computational Approach

RAS spectra are calculated as described in ref. [45,49-52]

$$\frac{\Delta R}{R} = \frac{16\pi\omega Z_S}{c} Im \frac{\alpha_{yy}(\omega) - \alpha_{xx}(\omega)}{\varepsilon_{Si}(\omega) - 1} \tag{2}$$

with the knowledge of the Si(553)–Au slab polarizability α_{ij} and the dielectric function of the silicon substrate ε_{Si}. Thereby x is the polarization direction perpendicular to the Au wires (e.g., $[11\bar{2}]$), while y is the direction parallel to the Au wires (e.g., $[1\bar{1}0]$). In Equation (2) c, is the light velocity in vacuum and Z_S the slab thickness.

The slab geometry and the optical response were calculated by DFT within the GGA in the revised Perdew–Burke–Ernzerhof (PBEsol) formulation.[53] The calculations had been performed with the Vienna ab initio Simulation Package (VASP).[54,55] Projector augmented waves (PAW) potentials[56,57] with projectors up to $l = 1$ for H ($1s^1$), $l = 2$ for Si ($3s^2 3p^2$) and $l = 3$ for Au ($5d^{10}6s^1$) were employed. A plane wave basis up to an energy cutoff of 410 eV and $4 \times 27 \times 1$ Monkhorst–Pack k-point meshes[58] were used.

The silicon surfaces are modeled with asymmetric slabs consisting of 6 Si bilayers stacked along the [111] crystallographic direction, the surface termination including the Au chains, and a vacuum region of about 20 Å. Hydrogen atoms saturated the dangling bonds at the lower face of the slabs. These atoms as well as the three lowest Si bilayers were frozen at their bulk position to model the substrate, while the remaining atoms were free to relax. Thereby, the atomic positions were relaxed until the residual Hellmann–Feynman forces are lower than 0.005 eV $Å^{-1}$.

The dimerization is quantified as usual by the dimensionless parameter

$$d = (|a_{Au} - a_{Si}|)/a_{Si} \tag{3}$$

where a_{Si} is the surface lattice constant and a_{Au} is the larger Au—Au bond length in the chain direction.

Acknowledgements

The authors gratefully acknowledge support from the Deutsche Forschungsgemeinschaft (research unit FOR1700). S.C. and J.P. acknowledge support from the Federal Ministry of Education and Research in the framework of the project CatLab (03EW0015A). Calculations for this research were conducted on the Lichtenberg high performance computer of the TU Darmstadt, and at Höchstleistungrechenzentrum Stuttgart (HLRS). The authors furthermore acknowledge the computational resources provided by the HPC Core Facility and the HRZ of the Justus-Liebig-Universität Gießen. The authors acknowledge financial support by the Ministerium für Kultur und Wissenschaft des Landes Nordrhein-Westfalen, Der Regierende Bürgermeister von Berlin - Senatskanzlei Wissenschaft und Forschung, and the Bundesministerium für Bildung und Forschung. The authors also acknowledge funding by the European Union through project EFRE 1.8/07: "High-resolution broad band spectroscopy."

Open Access funding enabled and organized by Projekt DEAL.

Conflict of Interest

The authors declare no conflict of interest.

Data Availability Statement

Research data are not shared.

Keywords

Au, DFT, infrared ellipsometry, reflectance anisotropy spectroscopy, Si(553), surface functionalization

Received: January 3, 2022
Revised: February 25, 2022
Published online: May 9, 2022

[1] H. W. Yeom, S. Takeda, E. Rotenberg, I. Matsuda, K. Horikoshi, J. Schaefer, C. M. Lee, S. D. Kevan, T. Ohta, T. Nagao, S. Hasegawa, *Phys. Rev. Lett.* **1999**, *82*, 4898.
[2] F. J. Himpsel, K. N. Altmann, R. Bennewitz, J. N. Crain, A. Kirakosian, J.-L. Lin, J. L. McChesney, *J. Phys.: Condens. Matter* **2001**, *13*, 11097.
[3] J. D. O'Mahony, J. F. McGilp, C. F. J. Flipse, P. Weightman, F. M. Leibsle, *Phys. Rev. B* **1994**, *49*, 2527.
[4] O. Gurlu, O. A. O. Adam, H. J. W. Zandvliet, B. Poelsema, *Appl. Phys. Lett.* **2003**, *83*, 4610.
[5] C. Zeng, P. Kent, T.-H. Kim, A.-P. Li, H. H. Weitering, *Nat. Mater.* **2008**, *7*, 539.
[6] I. Miccoli, F. Edler, H. Pfnür, S. Appelfeller, M. Dähne, K. Holtgrewe, S. Sanna, W. G. Schmidt, C. Tegenkamp, *Phys. Rev. B* **2016**, *93*, 125412.
[7] P. C. Snijders, H. H. Weitering, *Rev. Mod. Phys.* **2010**, *82*, 307.
[8] H. Weitering, *Nat. Phys.* **2011**, *7*, 744.
[9] C. Brand, H. Pfnür, G. Landolt, S. Muff, J. H. Dil, T. Das, C. Tegenkamp, *Nat. Commun.* **2015**, *6*, 8118.
[10] K. Holtgrewe, S. Appelfeller, M. Franz, M. Dähne, S. Sanna, *Phys. Rev. B* **2019**, *99*, 214104.
[11] T. Lichtenstein, Z. Mamiyev, E. Jeckelmann, C. Tegenkamp, H. Pfnür, *J. Phys. Condens. Matter* **2018**, *31*, 175001.
[12] S. Kagoshima, H. Nagasawa, T. Sambongi, *Electron Correlation And Magnetism In Narrow-Band Systems*, vol. *72*, Springer Series in Solid-State Sciences, Springer Berlin Heidelberg, Berlin, Heidelberg, **1988**.
[13] G. Grüner, *Rev. Mod. Phys.* **1988**, *60*, 1129.
[14] J. M. Luttinger, *J. Math. Phys.* **1963**, *4*, 1154.
[15] K. Schönhammer, *Luttinger Liquids: Basic concepts*, vol. *25*, Physics and Chemistry of Materials with Low-Dimensional Structures, ch. 4, Springer Netherlands, Dordrecht **2004**, pp. 93–136s.
[16] T. Giamarchi, *Quantum Physics in One Dimension*, Clarendon Press, Oxford, **2007**.
[17] J. N. Crain, J. L. McChesney, F. Zheng, M. C. Gallagher, P. C. Snijders, M. Bissen, C. Gundelach, S. C. Erwin, F. J. Himpsel, *Phys. Rev. B* **2004**, *69*, 125401.
[18] M. Krawiec, *Phys. Rev. B* **2010**, *81*, 115436.
[19] C. Braun, U. Gerstmann, W. G. Schmidt, *Phys. Rev. B* **2018**, *98*, 121402.
[20] S. Polei, P. C. Snijders, S. C. Erwin, F. J. Himpsel, K.-H. Meiwes-Broer, I. Barke, *Phys. Rev. Lett.* **2013**, *111*, 156801.
[21] S. Polei, P. C. Snijders, K.-H. Meiwes-Broer, I. Barke, *Phys. Rev. B* **2014**, *89*, 205420.
[22] J. Plaickner, E. Speiser, C. Braun, W. G. Schmidt, N. Esser, S. Sanna, *Phys. Rev. B* **2021**, *103*, 115441.
[23] S. C. Erwin, F. J. Himpsel, *Nat. Commun.* **2010**, *1*, 58.
[24] B. Hafke, T. Frigge, T. Witte, B. Krenzer, J. Aulbach, J. Schäfer, R. Claessen, S. C. Erwin, M. Horn-von Hoegen, *Phys. Rev. B* **2016**, *94*, 161403.
[25] J. Aulbach, S. C. Erwin, R. Claessen, J. Schäfer, *Nano Lett.* **2016**, *16*, 2698.
[26] C. Braun, S. Neufeld, U. Gerstmann, S. Sanna, J. Plaickner, E. Speiser, N. Esser, W. G. Schmidt, *Phys. Rev. Lett.* **2020**, *124*, 146802.
[27] B. Hafke, C. Brand, T. Witte, B. Sothmann, M. Horn-von Hoegen, S. C. Erwin, *Phys. Rev. Lett.* **2020**, *124*, 016102.
[28] C. Hogan, E. Speiser, S. Chandola, S. Suchkova, J. Aulbach, J. Schäfer, S. Meyer, R. Claessen, N. Esser, *Phys. Rev. Lett.* **2018**, *120*, 166801.
[29] S. Sanna, T. Lichtenstein, Z. Mamiyev, C. Tegenkamp, H. Pfnür, *J. Phys. Chem. C* **2018**, *122*, 25580.
[30] M. Tzschoppe, C. Huck, F. Hötzel, B. Günther, Z. Mamiyev, A. Butkevich, C. Ulrich, L. Gade, A. Pucci, *J. Phys. Condens. Matter* **2018**, *31*, 195001.
[31] F. Edler, I. Miccoli, J. P. Stöckmann, H. Pfnür, C. Braun, S. Neufeld, S. Sanna, W. G. Schmidt, C. Tegenkamp, *Phys. Rev. B* **2017**, *95*, 125409.
[32] Z. Mamiyev, M. Tzschoppe, C. Huck, A. Pucci, H. Pfnür, *J. Phys. Chem. C* **2019**, *123*, 9400.
[33] Z. Mamiyev, C. Fink, K. Holtgrewe, H. Pfnür, S. Sanna, *Phys. Rev. Lett.* **2021**, *126*, 106101.
[34] J. Aulbach, J. Schäfer, S. C. Erwin, S. Meyer, C. Loho, J. Settelein, R. Claessen, *Phys. Rev. Lett.* **2013**, *111*, 137203.
[35] Z. Mamiyev, S. Sanna, T. Lichtenstein, C. Tegenkamp, H. Pfnür, *Phys. Rev. B* **2018**, *98*, 245414.
[36] Z. Mamiyev, M. Tzschoppe, C. Huck, A. Pucci, H. Pfnür, *J. Phys. Chem. C* **2019**, *123*, 9400.
[37] Z. Mamiyev, S. Sanna, F. Ziese, C. Dues, C. Tegenkamp, H. Pfnür, *J. Phys. Chem. C* **2020**, *124*, 958.
[38] S. Suchkova, C. Hogan, F. Bechstedt, E. Speiser, N. Esser, *Phys. Rev. B* **2018**, *97*, 045417.
[39] S. Chandola, K. Hinrichs, M. Gensch, N. Esser, S. Wippermann, W. G. Schmidt, F. Bechstedt, K. Fleischer, J. F. McGilp, *Phys. Rev. Lett.* **2009**, *102*, 226805.
[40] C. Hogan, E. Ferraro, N. McAlinden, J. F. McGilp, *Phys. Rev. Lett.* **2013**, *111*, 087401.
[41] C. H. Patterson, S. Banerjee, J. F. McGilp, *Phys. Rev. B* **2016**, *94*, 165417.
[42] K. Christmann, *Surf. Sci. Rep.* **1988**, *9*, 1.
[43] C. Hogan, N. McAlinden, J. F. McGilp, *Phys. Status Solidi B* **2012**, *249*, 6.
[44] K. Biedermann, S. Regensburger, T. Fauster, F. J. Himpsel, S. C. Erwin, *Phys. Rev. B* **2012**, *85*, 245413.
[45] C. Hogan, M. Palummo, O. Pulci, C. M. Bertoni, *Surface Science*. Springer, Cham **2020**.
[46] J. Plaickner, E. Speiser, S. Chandola, N. Esser, D. K. Singh, *J. Raman Spectrosc.* **2020**, *51*, 788.
[47] S. W. Joo, S. W. Han, K. Kim, *J. Colloid Interface Sci.* **2001**, *240*, 391.
[48] D. E. Aspnes, A. A. Studna, *Phys. Rev. Lett.* **1985**, *54*, 1956.
[49] F. Manghi, R. Del Sole, A. Selloni, E. Molinari, *Phys. Rev. B* **1990**, *41*, 9935.
[50] C. Hogan, R. Del Sole, *Phys. Status Solidi B* **2005**, *242*, 3040.
[51] C. Hogan, N. McAlinden, J. F. McGilp, *Phys. Status Solidi B* **2012**, *249*, 1095.
[52] W. G. Schmidt, *Phys. Status Solidi B* **2005**, *242*, 2751.
[53] J. P. Perdew, A. Ruzsinszky, G. I. Csonka, O. A. Vydrov, G. E. Scuseria, L. A. Constantin, X. Zhou, K. Burke, *Phys. Rev. Lett.* **2008**, *100*, 136406.
[54] G. Kresse, J. Furthmüller, *Comput. Mater. Sci.* **1996**, *6*, 15.
[55] G. Kresse, J. Furthmüller, *Phys. Rev. B* **1996**, *54*, 11169.
[56] G. Kresse, D. Joubert, *Phys. Rev. B* **1999**, *59*, 1758.
[57] P. E. Blöchl, *Phys. Rev. B* **1994**, *50*, 17953.
[58] H. J. Monkhorst, J. D. Pack, *Phys. Rev. B* **1976**, *13*, 5188.